SCIENCE CHINA
Earth Sciences

•ARTICLE•

March 2025 Vol.68 No.3: 836–849
https://doi.org/10.1007/s11430-024-1509-3

Vegetation mapping of Yunnan Province by integrating remote sensing, field observations, and models

Mingjian XIAHOU[1†], Mingchun PENG[2†], Zehao SHEN[1,2*], Qingzhong WEN[3], Chongyun WANG[2], Yannan LIU[2], Qiuyuan ZHANG[2], Lei PENG[2], Changyuan YU[3], Xiaokun OU[2] & Jingyun FANG[1]

[1] *Key Laboratory of Ministry of Education for Earth Surface Processes, College of Urban & Environmental Sciences, Peking University, Beijing 100871, China*
[2] *School of Ecology and Environment, Yunnan University, Kunming 650504, China*
[3] *Yunnan Institute of Forest Inventory and Planning, Kunming 650051, China*

Received May 27, 2024; revised November 25, 2024; accepted January 3, 2025; published online February 14, 2025

Abstract Vegetation maps are crucial for ecologists and decision-makers, providing essential information on the spatial distribution of various vegetation types to support ecosystem exploration and management. Despite advancements in Earth observation and machine learning enabling large-scale vegetation mapping, creating detailed and accurate maps in biodiversity hotspots remains challenging due to significant environmental heterogeneity and frequent human disturbances. The lack of sufficient ground-based data and complex climate-vegetation interactions further limits mapping accuracy. In this study, we developed an integrated framework for multi-source data fusion to enhance vegetation mapping and validation in Yunnan Province, a global biodiversity hotspot region in Southwest China. The mapping process involved four key steps: (1) vegetation classification using random forest and Landsat imagery, (2) boundary calibration based on a locally calibrated static climate-vegetation model, (3) patch correction with independent forest inventory data, and (4) validation using adequate field observations. This approach enabled the mapping of 17 vegetation types and 44 subtypes in Yunnan Province (1:50000), categorized based on the growth-form composition of dominant species of the community. The overall accuracies were 0.747 and 0.710 for natural vegetation types and subtypes, and 0.905 and 0.891 for artificial types and subtypes. This high-resolution map enhances our understanding of vegetation distribution and ecological complexity in this region, offering valuable insights for policymakers to support conservation efforts and sustainable management strategies.

Keywords Vegetation mapping, Biodiversity hotspot region, Multi-source data, Data-fusion framework, Ecological diversity

Citation: Xiahou M, Peng M, Shen Z, Wen Q, Wang C, Liu Y, Zhang Q, Peng L, Yu C, Ou X, Fang J. 2025. Vegetation mapping of Yunnan Province by integrating remote sensing, field observations, and models. Science China Earth Sciences, 68(3): 836–849, https://doi.org/10.1007/s11430-024-1509-3

1. Introduction

Vegetation maps offer critical insights into the spatial distribution of ecosystems and land use types from local to global scales (Franklin, 1995; Pedrotti, 2012). They are essential for scientists and decision-makers, providing a solid foundation for geo-ecological studies and strategies for vegetation conservation, ecological restoration, and sustainable management (van der Maarel and Franklin, 2012; Liu et al., 2020). However, large-scale vegetation mapping and its updates can be challenging due to their high costs in terms of time and resources. Traditional mapping methods often involve manually delineating vegetation patch boundaries using contour topographic maps or aerial photographs, with

* Corresponding author (email: shzh@urban.pku.edu.cn)
† Equally contributed to this work.

vegetation types identified based on expert knowledge (Kuchler and Zonneveld, 1967; Roberts and Cooper, 1989). With the increasing impacts of global climate change and human activities, both natural and artificial vegetation are undergoing rapid transformations, introducing significant uncertainties in vegetation mapping (Gottfried et al., 2012; Fagan et al., 2018; Chen et al., 2019). Consequently, most traditional vegetation maps struggle to accurately represent current vegetation distributions and often fail to capture the dynamics of changing landscapes.

Advancements in Earth observation technologies and machine learning algorithms have made it possible to map large-scale vegetation distribution and monitor vegetation dynamics effectively (Xie et al., 2008; Adam et al., 2010; Gašparović and Dobrinić, 2020; Del Valle and Jiang, 2022). Remote sensing datasets, with their global coverage and free accessibility, significantly reduce the temporal and financial costs of large-scale vegetation mapping (Tong et al., 2023). These datasets provide detailed spectral information, including plant reflectance, texture, and phenology, which are crucial for accurate vegetation classification (Tuanmu et al., 2010; Verrelst et al., 2015; Madonsela et al., 2017). Beyond multispectral optical satellite bands, other datasets, including SAR (Grimaldi et al., 2020), LiDAR (Liang et al., 2020), and UAV imagery (de Castro et al., 2021), are also commonly employed in vegetation classification. Machine learning algorithms further enhance modern vegetation mapping by automatically identifying the nonlinear relationships between surface reflectance and land cover types. Popular algorithms include deep learning (DL) (Ienco et al., 2019), neural networks (Flood et al., 2019), decision trees (Tsai et al., 2018), support vector machine (SVM), and random forest (RF) classifiers. RF is widely used for both vegetation type classification and vegetation attribute regression, owing to its robust performance and efficiency in managing high-dimensional data and multicollinearity (van Beijma et al., 2014; Belgiu and Drăguţ, 2016). SVM can yield accurate maps with small training sample sizes, which is important given the challenges and costs associated with field data collection (Mountrakis et al., 2011; Shao and Lunetta, 2012). DL models require substantial data quality and quantity, such as hyperspectral high-resolution imagery and extensive training datasets, which can limit their application in large-scale vegetation mapping (Kattenborn et al., 2021).

Land Cover and Land Use (LCLU) maps serve as a useful foundation for detailed vegetation mapping (Hansen and Loveland, 2012), but the classification systems of existing LCLU maps are often too simplistic to capture information at the levels of vegetation type and subtype (Homer et al., 2015). Currently, vegetation maps with higher classification levels are available at various scales and regions. On a continental or national scale, a new version of China's vegetation map was updated using MODIS land surface products (Su et al., 2020). A seamless vegetation-type map of India was developed based on IRS LISS-III images (Roy et al., 2015). The circumpolar Arctic region's vegetation distribution was also revised, building upon the strengths of the original map (Walker et al., 2005; Raynolds et al., 2019). At a regional scale, Germany's agricultural areas were classified into 19 land cover classes using Sentinel-2 data (Preidl et al., 2020). Different rainforest vegetation types were mapped using maximum likelihood and random forest classification methods (Erinjery et al., 2018).

Despite advances in remote sensing and machine learning, detailed vegetation maps with fine spatial resolution and high accuracy remain scarce, particularly in regions with high environmental heterogeneity, rich biodiversity, and frequent human disturbances (Erinjery et al., 2018; Räsänen and Virtanen, 2019; Wagner et al., 2019). The main challenges include a lack of ground-based data, complex climate-vegetation interactions, indistinguishable forest types, and persistent human activity. Firstly, insufficient and unevenly distributed field sampling points present significant limitations for vegetation classification, making it difficult to train accurate and robust machine learning models (Treitz et al., 1992). Secondly, relying on a single data source is inadequate for detailed vegetation classification in biodiversity hotspots, where multiple vegetation types may share similar spectral signatures and phenological traits (Bioucas-Dias et al., 2013; Tsai et al., 2018). Thirdly, distinguishing secondary vegetation types that emerge following deforestation or afforestation is challenging (Carreiras et al., 2017; Chen et al., 2020). Moreover, although the distribution of agroecosystems is critical for ecosystem management, it is often overlooked in current vegetation mapping (Senf et al., 2013).

Yunnan, a province in southwestern China, forms a crucial part of one of the world's 36 global biodiversity hotspots (Myers et al., 2000). An accurate and detailed vegetation map is essential for effective biodiversity conservation and ecosystem management in this region (Li et al., 2015). However, topological variability, ecosystem diversity, and increasing human disturbance are three main constraints for vegetation mapping (Ye et al., 2020). The current vegetation map of Yunnan was created in the 1980s by traditional mapping approaches based on topographic contour maps, expert knowledge, and extensive field surveys (Wu and Zhu, 1987). The spatial resolution of this map is too low to reflect the details of vegetation distribution, and the accuracy of the map has not been systematically evaluated. Meanwhile, the spatial distribution of vegetation types has changed drastically in recent decades (Zomer et al., 2015; Shi and Chen, 2018; Sun et al., 2021). Therefore, there is an urgent need to produce an updated vegetation map with finer spatial resolution, more detailed classification, and higher mapping accuracy to reflect the current vegetation status in Yunnan.

The aim of this study is to investigate the complexity and

diversity of ecosystems in Yunnan by mapping the distribution of vegetation types. We utilize a multi-source data approach, incorporating remote sensing data, field observations, forest inventories, environmental factors, and expert knowledge. Specifically, our objectives were to (1) develop a data-fusion framework for vegetation mapping and validation in an ecologically diverse region using multiple data sources, (2) produce an accurate and up-to-date vegetation map for Yunnan, and (3) analyze the distribution patterns of vegetation types to provide recommendations for vegetation conservation and sustainable management.

2. Methods

2.1 Study area

The ecosystems of Yunnan are extremely diverse due to its drastic environmental variability and transitional location between three geographical regions (East Asia, Southeast Asia, and the Tibetan Plateau) (Figure 1). The environmental gradients from cold-wet alpine areas to dry-hot valleys provide diverse niches for plants and animals to survive drastic climate change (Wang et al., 2018). Tropical rainforests and evergreen broad-leaved forests formed by humid monsoons offer habitats to countless tropical species. Strongly disturbed by human activities, most ecosystems in central Yunnan are covered by secondary or artificial vegetation types. Karst geography shapes unique patterns of vegetation distribution in eastern Yunnan.

2.2 Classification system

The classification system was constructed mainly based on the *Ecosystems List of Yunnan Province* (Gao et al., 2021), which represents a cognitive update on *Yunnan Vegetation* three decades after Wu and Zhu (1987). Minor adjustments were made according to the field observation results. Finally, 17 vegetation types and 44 vegetation subtypes (32 natural vegetation subtypes, 9 artificial vegetation subtypes, and 3 non-vegetation subtypes) were included in this system (Appendix Table S1, https://link.springer.com).

2.3 Data sources

2.3.1 Remote sensing data

We obtained Landsat 8 OLI collection-2 Tier-1 level-2 surface reflectance images at 30-m resolution during 2018 and 2020 from USGS Earth Explorer (https://earthexplorer.usgs.gov/). After masking clouds and shadows, we first filtered the images by the date corresponding to three seasons: spring (March, April, and May), summer (June, July, and August), and autumn (September, October, November). Then we created composite seasonal mosaic images with the median method for six image bands (2-blue, 3-green, 4-red, 5-NIR,

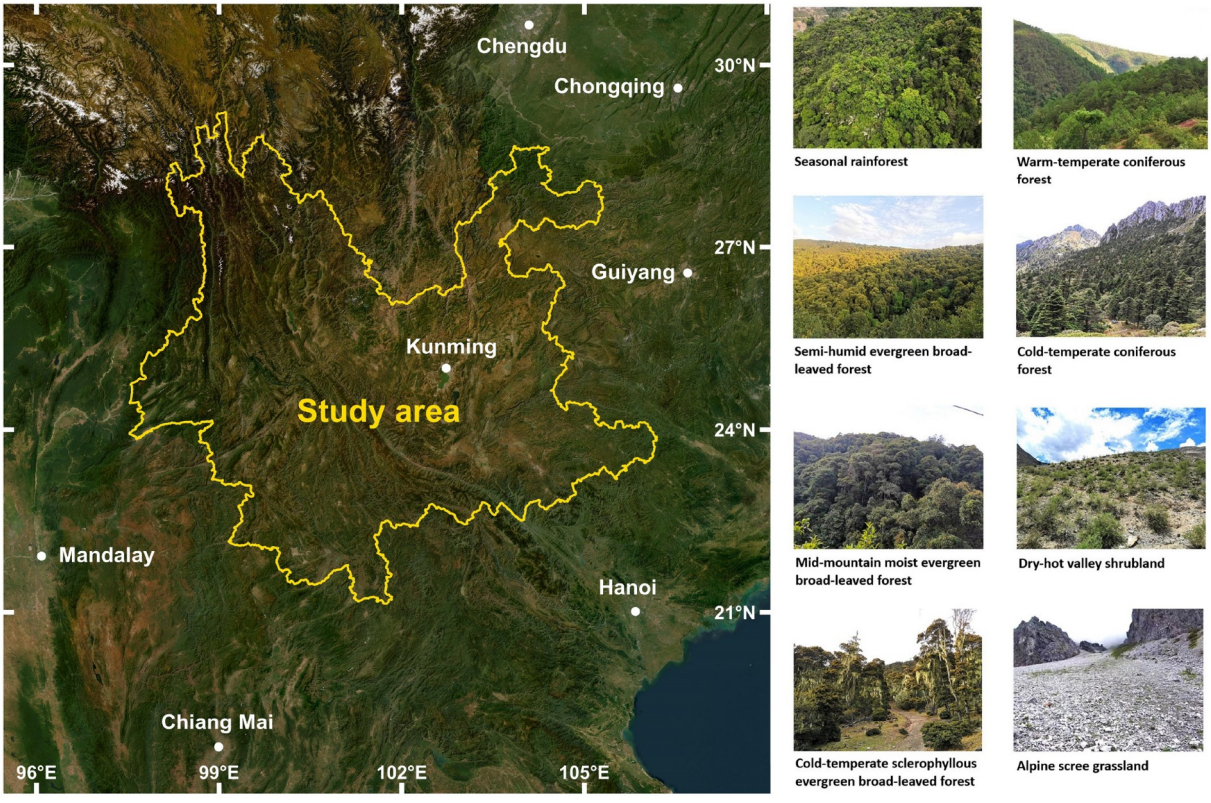

Figure 1 Study area and physiognomy of major vegetation types in Yunnan.

6-SWIR1, and 7-SWIR2), and calculated two vegetation indices (NDVI and EVI) with the mosaic images in each season. Photos from Google Earth at level 19 with a resolution of less than 1 m were used to support the visual interpretation of vegetation types. Additionally, four topological factors calculated from ASTER Global Digital Elevation at 30-m spatial resolution were included in the following analyses: elevation, slope, aspect, and roughness.

2.3.2 *Field data*

During 2018–2020, we collected more than 20000 field sample points and 5000 field plots throughout Yunnan. After one-by-one checking and screening, 15066 sample points and 2052 plots were selected for this study (Figure 2). The selected sample points are evenly distributed throughout Yunnan and cover all the 44 vegetation types in our classification system. The selected plots provided reliable references for map validation and covered 28 natural vegetation types. The investigation of original vegetation and plantations was carried out by the Yunnan Institute of Forest Inventory and Planning during 2010–2020, identifying and mapping the patches of original and artificial vegetation throughout Yunnan (Figure 2). Original vegetation patches refer to vegetation that is relatively old, has not been significantly disturbed by human activities, and retains its natural structures and functions. The identification and investigation of these original vegetation patches are detailed in Tao et al. (2016). Artificial vegetation patches refer to continuously managed plantations (e.g., rubber or eucalyptus plantations) or gardens (e.g., fruit orchards or tea gardens). These were all planted according to Yunnan's afforestation plans, which include both the extents and species of artificial vegetation patches. This independent investigation dataset not only marked the distribution area of original and artificial vegetation but also recorded the dominant species of most patches.

2.3.3 *Environmental factors and PNV map*

A potential natural vegetation (PNV) map was derived from the Comprehensive and Sequential Classification System (CSCS) with monthly climate data in Yunnan (Ren et al., 1980; Liang et al., 2012). Monthly mean temperature (MAT, °C) and monthly precipitation (MAP, cm) were interpolated with data from 184 meteorological stations in/around Yun-

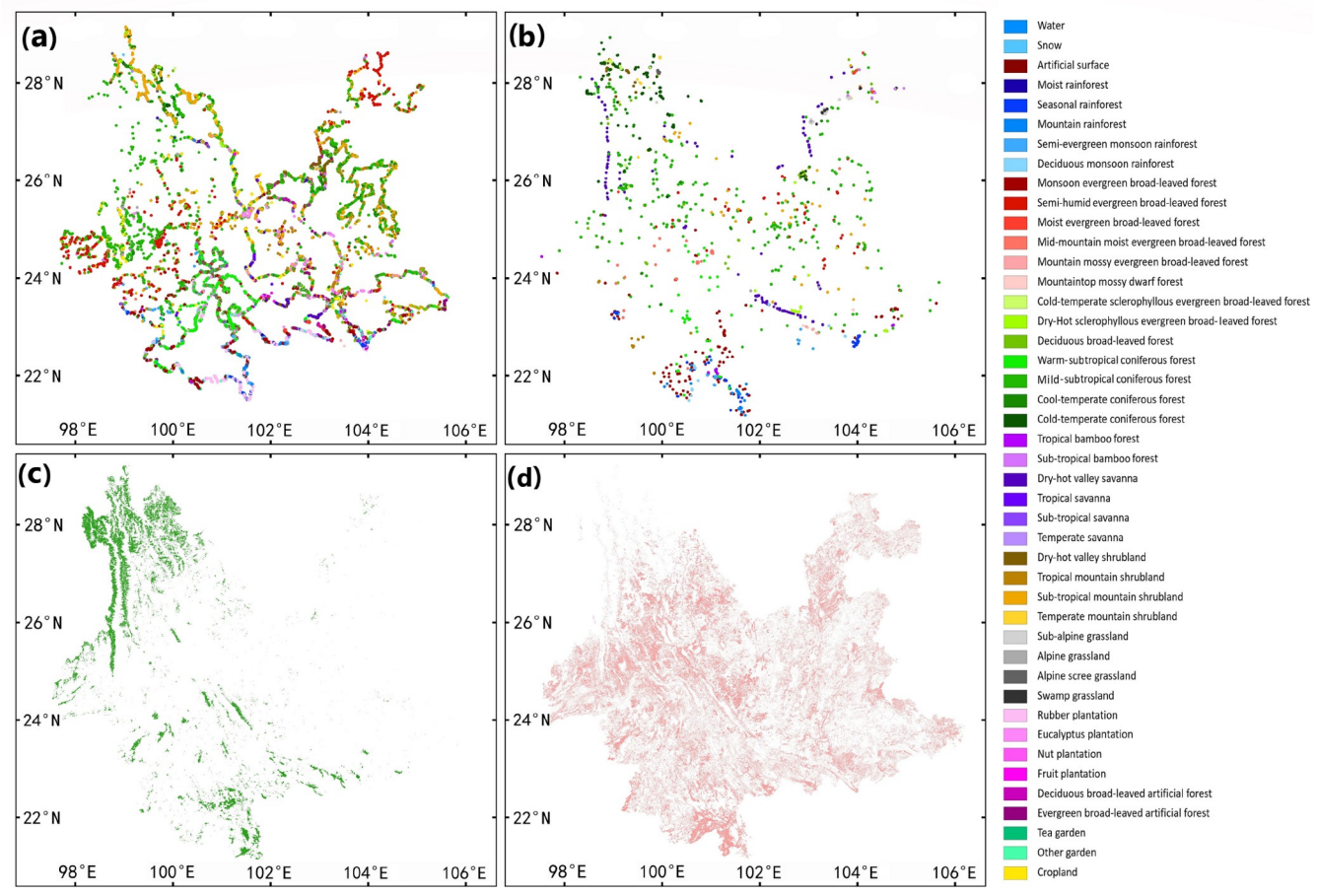

Figure 2 The spatial distribution of 15066 field sample points (a), 2052 natural vegetation plots (b), original vegetation patches (c), and artificial vegetation patches (d).

nan. The interpolation process was performed with thin plate smoothing splines in ANUSPLIN version 4.4, and DEM data were induced as a covariate factor (Hutchinson, 1995). Based on the accumulated temperature above 0°C (GDD0) and the degree of moisture (K), CSCS classified Yunnan into 17 potential vegetation types, which allowed us to set reliable climatic boundaries for vegetation types. We summarized the altitudinal and climatic boundaries of the 16 PNV types on 23 mountains in Yunnan according to 1930 field sample points collected from literatures, in order to refine the thresholds for heat (GDD0) and humidity (K) clustering of each PNV type. Details of the CSCS model and the PNV map are provided in Xiahou et al. (2024).

2.4 Data processing and validating

We employed a data-fusion-based framework to map and validate the distribution of vegetation types in Yunnan with various data sources (Figure 3). The systematic framework contained four major steps: (1) vegetation classification based on the random forest and Landsat images, (2) boundary calibration based on a locally calibrated climate-vegetation relationship (PNV map), (3) patch correction with independent forest inventory data, and (4) validation with adequate ground-based observations.

2.4.1 Vegetation classification

To track the best-performed method for vegetation classification, we compared the three most used algorithms for remote sensing vegetation classification, including Random Forest (RF), Support Vector Machine (SVM), and Deep Learning (DL). The 15066 sample points were randomly divided into a training dataset (70%) and a test dataset (30%) to train and test the performance of three models. After the trial tests, we fitted (1) an RF model with 1000 trees and 5 random variables at each split, (2) an SVM model with linear

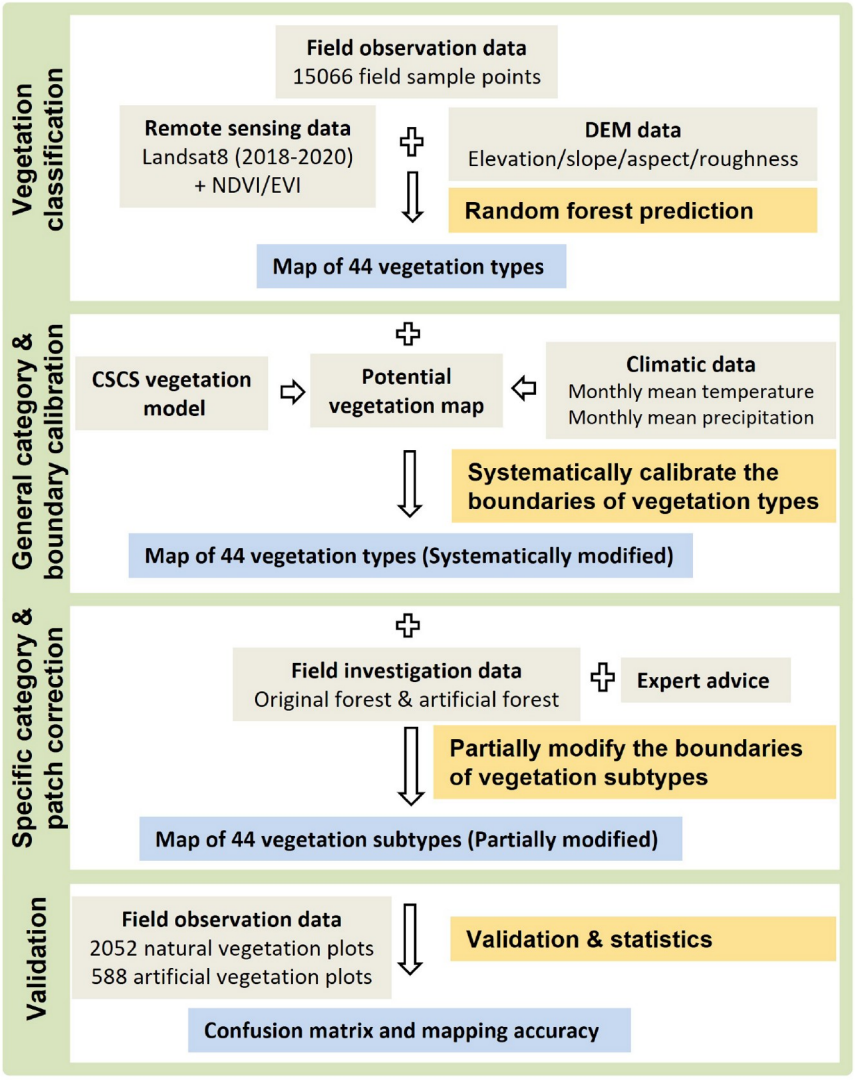

Figure 3 Workflow for mapping vegetation types with multi-source data.

kernel, and (3) a DL model with 8 hidden layers (with 128 neurons each) and input/output layers (with softmax action). Results showed that the RF model has the highest classification accuracy for our dataset. Therefore, we finally used the random forest algorithm to classify vegetation in Yunnan. Training data for the model were 15066 selected field sample points.

2.4.2 General category & boundary calibration

We systematically adjusted the climatic boundaries of zonal vegetation types according to the PVN map, which is an ideal reference for boundary modification since it integrated both climatic limitations and empirical knowledge about the environmental ranges of zonal vegetation types. Specifically, we compared the potential and realistic spatial distribution of each zonal vegetation type and modified the vegetation patches located outside the potential distribution area to the corresponding potential vegetation types. This step was especially useful in distinguishing vegetation types with similar appearance and spectral characteristics but distributed in different climatic and geographic zones.

2.4.3 Specific category & patch correction

We masked the vegetation map with the original and artificial vegetation patches obtained from the field forest inventory data. Unmatched regions were directly modified according to the inventory data because it was difficult to recognize specific forest types by remote sensing, and the forest inventory data were generated by reliable field surveys. Expert advice was also considered when we manually inspected and partially adjusted the vegetation map because knowledge about the species composition, community structure, succession process, causes of formation, and plant flora was extremely important for understanding and modelling the spatial distribution of vegetation types. Visual inspection helps us improve the accuracy of transitional and non-typical vegetation types in complex ecosystems like tropical/subtropical regions. Moreover, we incorporated patches smaller than 5 ha into their neighbors for the final map presentation, because in field surveys we found that the distribution of vegetation types often has a certain degree of continuity, and vegetation patches smaller than 5 ha are rare and unstable.

2.4.4 Validation & cartographic synthesis

Accuracies of the Yunnan vegetation map were evaluated at the vegetation type and subtype levels. Reference data comprised 2052 natural vegetation plots and 588 artificial vegetation plots with detailed information about the vegetation communities in Yunnan to calculate the overall accuracy, the precision of each vegetation type and subtype, and the recall. We used the field plots since they are more carefully investigated than the field sample points. Overall accuracy refers to the ratio of correctly classified field plots to the total number of field plots. Precision is the ratio of correctly classified field plots for a specific vegetation type to the total number of plots predicted to be that type. Recall is the ratio of correctly classified field plots to the total number of field plots of that type. Data processing in this study was based on QGIS 3.16, R 4.0, Google Earth Engine, and ANUSPLIN 4.4.

3. Results

3.1 Vegetation map adjusted with ground-based data

The overall classification accuracies for RF, SVM, and DL were 0.518, 0.458, and 0.371, respectively. RF showed the best performance in vegetation classification for our datasets. The accuracies of RF and SVM were acceptable considering a large number of vegetation types (44 types) and a limited training dataset in such a large area. Besides, many types share similar spectral and terrain characteristics, which makes it difficult to classify precisely by remote sensing images at the level of vegetation subtypes. However, the classification can be right at the level of vegetation types or vegetation groups, setting a good foundation for boundary calibration and patch correction.

Overall, 48.41% (179117 km^2) of the total area in Yunnan was modified through boundary calibration and patch correction. Among these changes, 25.54% (94498 km^2) was corrected by field investigation data of original and artificial vegetation, making the greatest contributions to map improvements. 14.37% (53169 km^2) of the total area was calibrated by PVN map mainly at the subtype level. The rest 8.5% (31450 km^2) was corrected according to expert advice and manual inspection, which mainly targeted at some special vegetation types and special regions.

3.2 Spatial distribution of vegetation types in Yunnan Province

The most extensive vegetation type in Yunnan is the mid-subtropical coniferous forest (primarily *Pinus yunnanensis*), covering approximately 103108 km^2. This forest is widely distributed across the province, extending from southern subtropical areas to the northwestern mountains, with a significant presence on the Central Yunnan Plateau (Figure 4a). Another key natural vegetation type on the Plateau is the semi-humid evergreen broad-leaved forest (4191 km^2), much of which has been degraded due to human activity and fire disturbances. Cropland, covering around 82448 km^2, is the second most widespread vegetation type in Yunnan, primarily found in intermountain basins and gentle foothills, underscoring the region's agricultural importance. Following these are three subtropical vegetation types located in Yun-

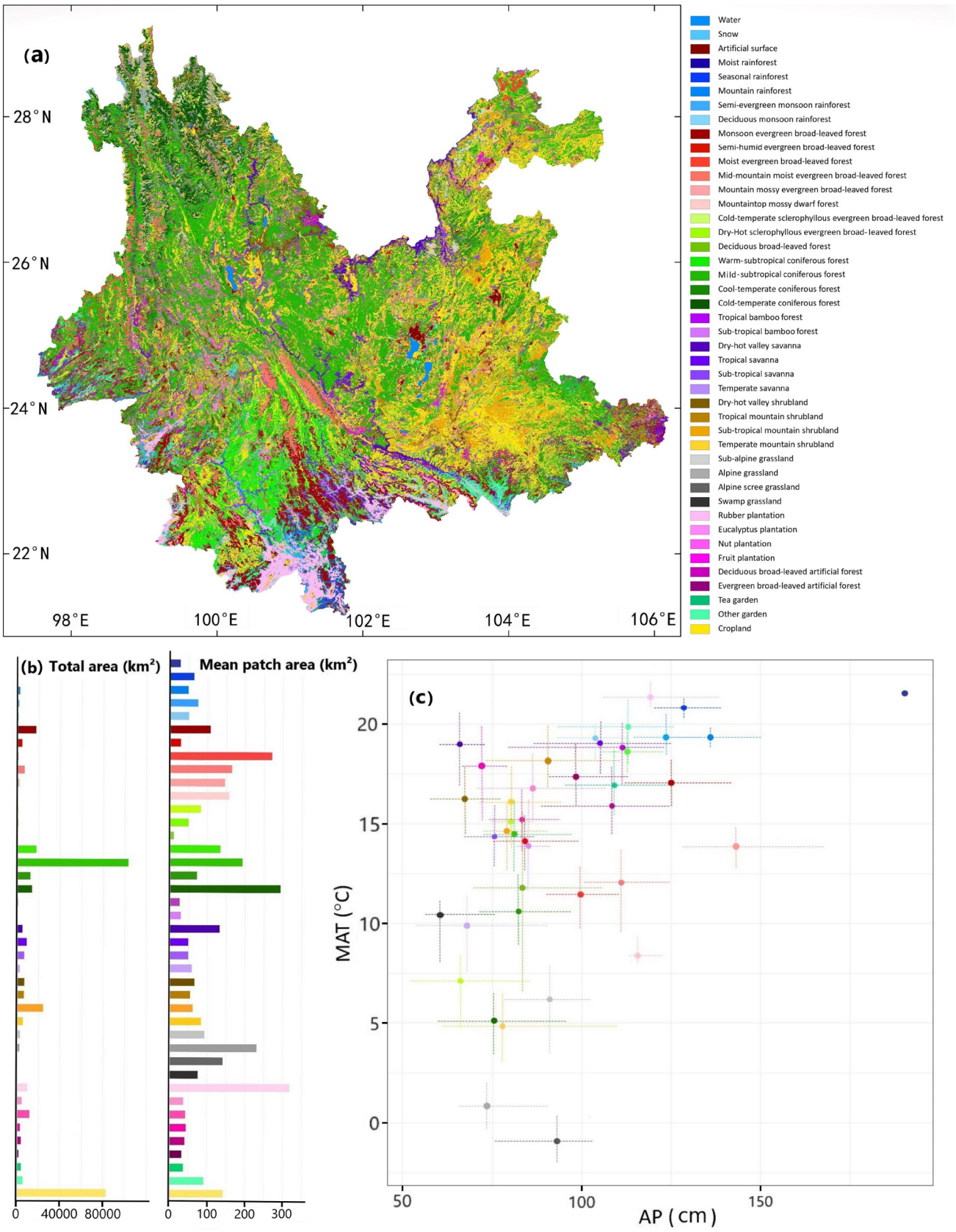

Figure 4 Map of Yunnan vegetation 44 subtypes after modification (a), total area and patch area (b), and environmental range of vegetation subtypes along MAT (Mean Annual Temperature) and AP (Annual Precipitation) axes (c).

nan's southern mountains: tropical and subtropical mountain shrubland (33113 km^2), warm-tropical coniferous forest (17626 km^2), and monsoon evergreen broad-leaved forest (17023 km^2). In northwestern Yunnan, cool-temperate coniferous forest (12182 km^2, mostly *Pinus armandii*) and cold-temperate coniferous forest (13749 km^2, mostly *Picea* and *Abies*), along with temperate mountain shrubland (5451 km^2) and meadows (5734 km^2), form the vertical vegetation gradient of the mid-to-upper slopes of the Hengduan Mountains. In southern Yunnan, mid-mountain moist evergreen broad-leaved forest (6390 km^2) and mountain mossy evergreen broad-leaved forest (1533 km^2) are significant natural vegetation types in the warm and humid mountain regions. Rainforest, covering approximately 3029 km^2 and characterized by dense, diverse flora, is concentrated in tropical valleys with favorable moisture conditions. Deciduous (1178 km^2) and semi-evergreen (1652 km^2) monsoon rainforests are prevalent in wide valleys influenced by the monsoon climate. The dry-hot valley savanna (5130 km^2) is a distinctive vegetation type found in deep valleys perpendicular to the summer monsoon direction. Among artificial forests, nut plantations are the largest, covering around 11836 km^2, followed by rubber plantations (9706 km^2), which are predominantly found in the southern tropical regions where rubber cultivation is prominent.

Patch area indicates the degree of fragmentation among vegetation types. The largest patch areas for natural vegetation are found in three alpine types: cold-temperate coniferous forests, moist evergreen broad-leaved forests, and alpine meadows (Figure 4b). In contrast, low-altitude vegetation types, such as deciduous broad-leaved forests and moist rainforests, have smaller patch areas. Among artificial vegetation, rubber plantations, and cropland have larger patches compared to other plantations and gardens.

Regarding the environmental range of vegetation types, most prefer moderate temperatures (around 15°C) and precipitation (around 80 cm), including the dominant warm-temperate coniferous forest and cropland (Figure 4c). Tropical vegetation types, such as rainforests and rubber plantations, occupy the hottest and most humid regions. Evergreen broad-leaved forests also thrive in areas with high precipitation but prefer cooler temperatures than rainforests. Alpine regions are dominated by cold-adapted vegetation, including meadows, temperate mountain shrubland, and cold-temperate coniferous forests.

3.3 Accuracy assessment

The overall accuracies of natural vegetation types and subtypes are 0.747 and 0.710, respectively (Table 1; Appendix Table S2). For artificial vegetation types and subtypes, the overall accuracies are 0.905 and 0.891, respectively (Table 2; Appendix Table S3). In general, the overall accuracy for artificial vegetation types is much higher than the accuracy of natural vegetation types. The widespread zonal vegetation types showed higher accuracy than fragmented and secondary vegetation types in our vegetation map. Among all natural vegetation types, sub-alpine meadow, dry-hot valley shrubland, and dry-hot valley savanna have the largest mapping accuracies (above 0.8). Accuracies of most evergreen broad-leaved forest types and coniferous forest types exceed 0.7, higher than the average mapping accuracy of other vegetation types. The accuracies of rainforest types are around 0.6, which is lower than the average accuracy but still acceptable since mapping the distribution of rainforests is always a great challenge. Accuracies of fragmented and secondary vegetation types are lower than expected, such as sclerophyllous evergreen broad-leaved forests, deciduous broad-leaved forests, and bamboos.

3.4 Detailed maps of vegetation types

We used five 30 km×30 km examples across Yunnan to present the details of our final vegetation map and compared these to the preliminary vegetation map before modification and the vegetation map for the 1980s. In general, our ultimate map after the systematic and patch correction showed more details than the other two maps (Figure 5). Specifically, in alpine areas, our map not only divided meadow and coniferous forest into more detailed types but also recognized more sub-alpine shrubland and sclerophyllous evergreen broad-leaved forests. In the tropics, the distribution of plantations and gardens was better mapped with our ultimate map than the other two maps. Around cities, we made great efforts to distinguish different artificial land uses and modify the misclassified patches. Additionally, vegetations in karst hills and dry-hot valleys were particularly focused on.

4. Discussion

4.1 Accuracies of Yunnan vegetation map

This study generated a practical framework for vegetation mapping and validating in a global biodiversity hotspot with high ecologically complex. The overall accuracies were 0.747 and 0.710 for natural vegetation type and subtypes, and 0.905 and 0.891 for artificial vegetation type and subtypes. Research has shown that the accuracies of vegetation maps are strongly related to spatial resolution, classification system, and study area, besides data sources and mapping approaches (Xie et al., 2008; Räsänen and Virtanen, 2019). This study attempted to find a balanced method between spatial resolution, classification system, mapping accuracy, and mapping efficiency, to comprehensively reflect the distribution of heterogeneous vegetation types and complex

Table 1 Recall and precision of natural vegetation types and subtypes

Vegetation type	Number	Recall	Precision	Vegetation subtype	Number	Recall	Precision
Rainforest	110	0.71	0.83	Seasonal rainforest	71	0.61	0.74
				Mountain rainforest	39	0.59	0.64
Monsoon rainforest	34	0.59	0.38	Semi-evergreen monsoon rainforest	19	0.53	0.30
				Deciduous monsoon rainforest	15	0.47	0.37
Evergreen broad-leaved forest	412	0.76	0.83	Monsoon evergreen broad-leaved forest	179	0.71	0.82
				Semi-humid evergreen broad-leaved forest	137	0.75	0.83
				Moist evergreen broad-leaved forest	15	0.60	0.47
				Mid-mountain moist evergreen broad-leaved forest	56	0.73	0.71
				Mountain mossy evergreen broad-leaved forest	16	0.69	0.85
				Mountaintop mossy dwarf forest	8	0.75	1.00
Sclerophyllous evergreen broad-leaved forest	59	0.53	0.76	Cold-temperate sclerophyllous evergreen broad-leaved forest	21	0.54	0.73
				Dry-hot sclerophyllous evergreen broad-leaved forest	35	0.51	0.78
Deciduous broad-leaved forest	56	0.10	0.63	Deciduous broad-leaved forest	56	0.10	0.63
Sub-tropical coniferous forest	474	0.74	0.74	Warm-subtropical coniferous forest	48	0.65	0.69
				Mild-subtropical coniferous forest	426	0.75	0.74
Temperate coniferous forest	350	0.83	0.93	Cool-temperate coniferous forest	96	0.71	0.70
				Cold-temperate coniferous forest	253	0.76	0.90
Bamboo forest	22	0.41	0.69	Tropical bamboo forest	15	0.40	0.75
				Sub-tropical bamboo forest	7	0.43	0.60
Savanna	138	0.83	0.74	Dry-hot valley savanna	140	0.80	0.95
Shrubland	167	0.69	0.60	Dry-hot valley shrubland	30	0.69	0.66
				Tropical mountain shrubland	35	0.51	0.78
				Sub-tropical mountain shrubland	39	0.67	0.51
				Temperate mountain shrubland	57	0.72	0.51
Meadow	235	0.88	0.88	Sub-alpine meadow	172	0.87	0.86
				Alpine meadow	14	0.76	0.43
				Alpine scree meadow	14	0.79	1.00
				Swamp meadow	27	0.52	0.82
Overall accuracy		0.747		Overall accuracy		0.710	

ecosystems in this provincial biodiversity hotspot region.

At the continental scale, vegetation map classification systems tend to be comprehensive but have coarse spatial resolutions due to computational constraints. These maps typically have lower mapping accuracies compared to our map, as they cover large areas with heterogeneous environments and complex vegetation types (Roy et al., 2015; Raynolds et al., 2019). For instance, the overall accuracies of the updated vegetation map of China are 64.8% at the vegetation type group level and 61% at the vegetation type/subtype level (Su et al., 2020). At the regional scale, many studies have produced vegetation maps with high spatial resolution and mapping accuracy. For example, the distribution of five types of rainforests and tropical plantations was mapped with 75% accuracy (Erinjery et al., 2018). A land use map of the Sahel region achieved an overall accuracy of 72%±3.9% (Schulz et al., 2021), and 24 vegetation types in Western Australia were classified with 74% accuracy (Macintyre et al., 2020). However, the application of these maps is often limited by their simple classification systems and small mapping extents (Li et al., 2020; Lopes et al., 2020). At the provincial scale, the accuracy of vegetation

Table 2 Recall and precision of artificial vegetation types and subtypes

Vegetation type	Number	Recall	Precision	Vegetation subtype	Number	Recall	Precision
Cropland	249	0.91	0.99	Cropland	249	0.91	0.99
Plantation	237	0.89	0.94	Rubber plantation	39	0.92	0.97
				Eucalyptus plantation	43	0.93	0.95
				Nut plantation	29	0.79	0.85
				Fruit plantation	21	0.95	0.76
				Other deciduous broad-leaved plantation	29	0.82	0.92
				Other evergreen broad-leaved plantation	76	0.86	0.91
Garden	102	0.86	0.92	Tea garden	48	0.89	0.93
				Other gardens	54	0.81	0.89
Overall accuracy		0.905		Overall accuracy		0.891	

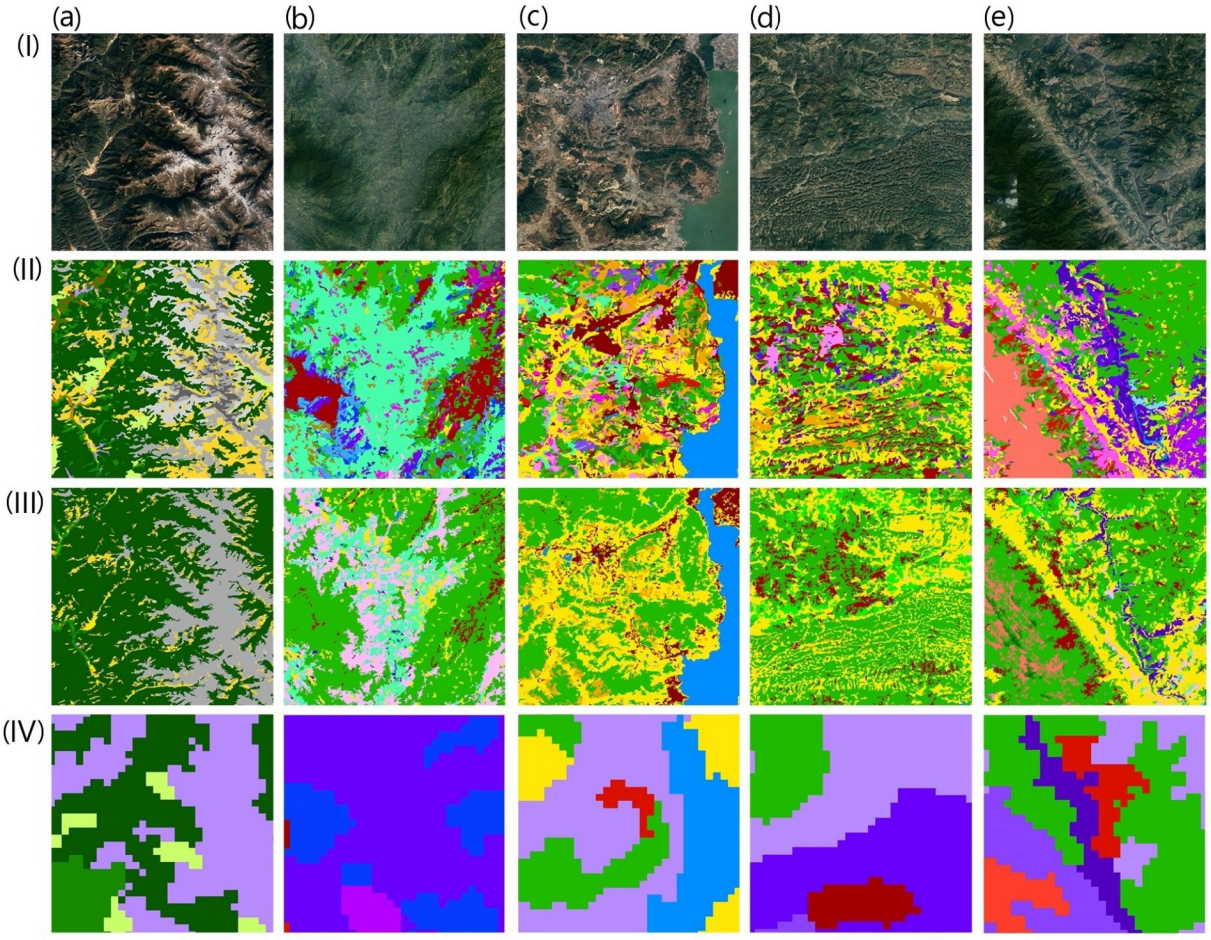

Figure 5 A comparison of vegetation details in five areas in Yunnan reflected by remote sensing images and different vegetation maps: Google Earth image (I), ultimate vegetation map (II), preliminary vegetation map (III), and vegetation map in "Yunnan Vegetation" in the 1980s (IV). The colors of the vegetation types are shown in Figure 4. Locations of these five examples were showed in Appendix Figure S2.

maps largely depends on the complexity of the vegetation and environment in the study area. Regions with homogeneous environments and low biodiversity tend to have high mapping accuracy, while more complex and biodiverse areas show lower accuracy (Zhang et al., 2019; Ghorbanian et al., 2020; Liu et al., 2020; Preidl et al., 2020).

4.2 Advantages and shortages of the data-fusion-based mapping approach

The relatively high accuracy of our map is mainly due to various data sources, data-fusion-based mapping approaches, and a comprehensive understanding of Yunnan vegetation (Del Valle and Jiang, 2022). Compared with single-data-source vegetation mapping, our data-fusion-based mapping framework and various data sources generated more comprehensive and accurate vegetation maps, considering the diverse and complicated vegetation communities in Yunnan (Ran et al., 2012; Zhang and Xie, 2014; Yao et al., 2020). We solved the problem that multiple vegetation types share similar spectral signatures, overcoming the shortage of using only remote sensing data. Sufficient ground-based data are the foundation for accurate vegetation mapping and validating, even with higher quality remote sensing images and updated classification algorithms. In this study, 15066 field sample points throughout the research area are used as train data for the random forest algorithm, which is more sufficient and reliable than most vegetation maps (Lopes et al., 2020; Wu et al., 2021). This ensures the robustness of the algorithm and the accuracy of classification. Forest inventory data also help us refine the details of our vegetation map by distinguishing the subtypes of forest (original forest & secondary forest, natural forest & plantation) and recognizing tree species of gardens (tea & fruit & nut) and plantations (rubber & eucalyptus, etc.), which are significant for vegetation conservation and sustainable management but often ignored in vegetation maps (Trisasongko and Paull, 2020; Azizan et al., 2021). We also incorporated temperature and precipitation into the vegetation map by the CSCS model and PNV map, instead of treating them as environmental factors, since the relationship between vegetation distribution and climate conditions in Yunnan is complex, thus cannot be simply simulated (Biermann, 2007; Ni and Herzschuh, 2011; Zhu et al., 2016; Fan and Bai, 2021). In the CSCS model, accumulated temperature, humidity index, and their interactions were considered, as well as the empirical knowledge about the distribution of zonal vegetation types (Liang et al., 2012; Du et al., 2022). The thresholds between different vegetation types were carefully adjusted, and the accuracies of the PNV map were evaluated according to field data and expert advice. Therefore, the PNV map offered a more systematic and robust reference to adjust the climatic boundaries for zonal vegetation types.

However, we also noticed that the accuracies of some vegetation types still need to be improved. It was difficult to accurately classify transitional, secondary, fragmented, and scattered vegetation types. For transitional and non-typical vegetation types like monsoon rainforest, it is difficult to define and recognize the key features by remote sensing images and vegetation-climate models. More knowledge about plant taxonomy and flora is needed to improve the accuracy. For secondary vegetation types like savanna, their appearance and distribution are diverse and unstable due to the frequent natural or artificial disturbances, which brings higher requirements on the quantity and quality of field data for accurate classification. For fragmented and scattered vegetation types such as deciduous broad-leaved forests and bamboo, specifically targeted field surveys are inevitable for future improvements.

4.3 Vegetation distribution and biodiversity conservation

This study reveals the environmental heterogeneity, ecological complexity, and biodiversity of Yunnan through its vegetation distribution. Basically, the climate gradients, ranging from tropical (MAT > 25°C) to cold (MAT < −5°C), and from humid (AP > 2000 mm) to arid (AP < 500 mm), fundamentally shape the diversity of vegetation types, which in turn drives overall biodiversity. Horizontally, the unique terrain, with lower elevations in the south and higher in the north, creates a distinct zonation of climate and vegetation. Southern Yunnan is characterized by rainforests, monsoon rainforests, and monsoon evergreen broad-leaved forests. The central Yunnan plateau hosts semi-humid evergreen broad-leaved forests and mid-temperate coniferous forests, while cold-temperate coniferous forests dominate the northwestern mountains. Vertically, Yunnan's fragmented landscape, with alternating mountains and valleys, results in pronounced mountainous vegetation zones. In southern Yunnan, vegetation transitions from moist rainforests in the valleys to mountain rainforests, monsoon evergreen broad-leaved forests, mid-mountain moist evergreen broad-leaved forests, mountain mossy evergreen broad-leaved forests, and mountain-top mossy dwarf forests at higher elevations. In the northwest, vegetation ranges from dry-hot valley savannas to temperate coniferous forests, mountain shrublands, and alpine meadows. Furthermore, Yunnan's vegetation exhibits significant transitional characteristics due to the simultaneous influence of the southwestern and southeastern summer monsoons. The southwestern monsoon primarily affects the southern region, leading to vegetation similar to that of the Indochina Peninsula, while the southeastern monsoon shapes the eastern region's vegetation, making it resemble that of the South China monsoon region.

Our vegetation map also illustrates specific regions and vegetation types that need to be focused on in biodiversity conservation and ecosystem management. Attention should be paid to highly fragmented and disturbed vegetation types with small patch areas, such as rainforests and seasonal rainforests. These vegetation types are seriously threatened by drastic climate changes and frequent human activities and are difficult to restore after destruction (Taubert et al., 2018;

Liu et al., 2019). Secondary vegetation types are usually in the transitional state of short-term vegetation recovery after the destruction of the natural forest. By reducing human disturbance and increasing protection measurements, these types have the potential to succeed toward the advanced plant communities and thus impact ecosystem services and the carbon cycle in the future (Wang et al., 2017; Zeng et al., 2019). Furthermore, the conservation of natural vegetation types with climax community structure should not be neglected. These vegetation types provide important habitats and refuges for plants and animals to avoid disturbance (Verrall and Pickering, 2020).

5. Conclusion

This study mapped the spatial distribution of vegetation types in Yunnan Province (1:50000), highlighting the complexity and diversity of its ecosystems. We developed a new data-fusion approach that integrates multiple data sources to address the challenges of large-scale remote sensing vegetation mapping in biodiversity hotspot regions. Specifically, we (1) utilized extensive ground-based observations to provide representative training data for the random forest classifier and reliable references for map validation, (2) modeled the climate-vegetation relationships to systematically refine vegetation type boundaries, (3) incorporated independent forest inventory data to differentiate detailed forest types, and (4) used forestry planning data to map artificial ecosystems. Consequently, the spatial distribution of 17 vegetation types and 44 subtypes in Yunnan. The overall accuracies were 0.747 and 0.710 for natural vegetation types and subtypes, and 0.905 and 0.891 for artificial types and subtypes. With a 30 m spatial resolution, this map offers detailed, reliable, and spatially precise information, supporting further exploration of ecosystem properties and providing a solid foundation for biodiversity conservation and sustainable ecosystem management.

Acknowledgements *We thank Tao YANG, Yanjie ZUO, Wei MENG, Fuli LI, Jianghua DUAN, Lina REN, Xiuli SU, and Ya KANG for their contributions to the field sampling points survey. This work was supported by the Major Program for Basic Research Project of Yunnan Province (Grant No. 202101BC070002) and the Second Comprehensive Scientific Expedition of the Tibetan Plateau (Grant No. 2019QZKK04020101).*

Conflict of interest The authors declare that they have no conflict of interest.

References

Adam E, Mutanga O, Rugege D. 2010. Multispectral and hyperspectral remote sensing for identification and mapping of wetland vegetation: A review. Wetlands Ecol Manage, 18: 281–296

Azizan F A, Kiloes A M, Astuti I S, Abdul Aziz A. 2021. Application of optical remote sensing in rubber plantations: A systematic review. Remote Sens, 13: 429

Belgiu M, Drăguţ L. 2016. Random forest in remote sensing: A review of applications and future directions. ISPRS J Photogramm Remote Sens, 114: 24–31

Biermann F. 2007. 'Earth system governance' as a crosscutting theme of global change research. Glob Environ Change, 17: 326–337

Bioucas-Dias J M, Plaza A, Camps-Valls G, Scheunders P, Nasrabadi N, Chanussot J. 2013. Hyperspectral remote sensing data analysis and future challenges. IEEE Geosci Remote Sens Mag, 1: 6–36

Carreiras J M B, Jones J, Lucas R M, Shimabukuro Y E. 2017. Mapping major land cover types and retrieving the age of secondary forests in the Brazilian Amazon by combining single-date optical and radar remote sensing data. Remote Sens Environ, 194: 16–32

Chen C, Park T, Wang X, Piao S, Xu B, Chaturvedi R K, Fuchs R, Brovkin V, Ciais P, Fensholt R, Tømmervik H, Bala G, Zhu Z, Nemani R R, Myneni R B. 2019. China and India lead in greening of the world through land-use management. Nat Sustain, 2: 122–129

Chen J, Yan F, Lu Q. 2020. Spatiotemporal variation of vegetation on the Qinghai-Tibet Plateau and the influence of climatic factors and human activities on vegetation trend (2000–2019). Remote Sens, 12: 3150

de Castro A I, Shi Y, Maja J M, Peña J M. 2021. UAVs for vegetation monitoring: Overview and recent scientific contributions. Remote Sens, 13: 2139

Del Valle T M, Jiang P. 2022. Comparison of common classification strategies for large-scale vegetation mapping over the Google Earth Engine platform. Int J Appl Earth Obs Geoinf, 115: 103092

Du H, Zhao J, Shi Y. 2022. Spatio-temporal distribution of sensitive regions of potential vegetation in China based on the Comprehensive Sequential Classification System (CSCS) and a climate-change model. Rangeland J, 43: 353–361

Erinjery J J, Singh M, Kent R. 2018. Mapping and assessment of vegetation types in the tropical rainforests of the Western Ghats using multispectral Sentinel-2 and SAR Sentinel-1 satellite imagery. Remote Sens Environ, 216: 345–354

Fagan M E, Morton D C, Cook B D, Masek J, Zhao F, Nelson R F, Huang C. 2018. Mapping pine plantations in the southeastern U.S. using structural, spectral, and temporal remote sensing data. Remote Sens Environ, 216: 415–426

Fan Z, Bai X. 2021. Scenarios of potential vegetation distribution in the different gradient zones of Qinghai-Tibet Plateau under future climate change. Sci Total Environ, 796: 148918

Flood N, Watson F, Collett L. 2019. Using a U-net convolutional neural network to map woody vegetation extent from high resolution satellite imagery across Queensland, Australia. Int J Appl Earth Obs Geoinf, 82: 101897

Franklin J. 1995. Predictive vegetation mapping: Geographic modelling of biospatial patterns in relation to environmental gradients. Prog Phys Geog, 19: 474–499

Gao Z, Sun H, Ou X. 2021. Ecosystems List of Yunnan Province (in Chinese). Kunming: Yunnan Scientific Publishing Press

Gašparović M, Dobrinić D. 2020. Comparative assessment of machine learning methods for urban vegetation mapping using multitemporal Sentinel-1 imagery. Remote Sens, 12: 1952

Ghorbanian A, Kakooei M, Amani M, Mahdavi S, Mohammadzadeh A, Hasanlou M. 2020. Improved land cover map of Iran using Sentinel imagery within Google Earth Engine and a novel automatic workflow for land cover classification using migrated training samples. ISPRS J Photogramm Remote Sens, 167: 276–288

Gottfried M, Pauli H, Futschik A, Akhalkatsi M, Barančok P, Benito Alonso J L, Coldea G, Dick J, Erschbamer B, Fernández Calzado M ı R, Kazakis G, Krajči J, Larsson P, Mallaun M, Michelsen O, Moiseev D, Moiseev P, Molau U, Merzouki A, Nagy L, Nakhutsrishvili G, Pedersen B, Pelino G, Puscas M, Rossi G, Stanisci A, Theurillat J P, Tomaselli M, Villar L, Vittoz P, Vogiatzakis I, Grabherr G. 2012. Continent-wide response of mountain vegetation to climate change. Nat Clim Change, 2: 111–115

Grimaldi S, Xu J, Li Y, Pauwels V R N, Walker J P. 2020. Flood mapping

under vegetation using single SAR acquisitions. Remote Sens Environ, 237: 111582
Hansen M C, Loveland T R. 2012. A review of large area monitoring of land cover change using Landsat data. Remote Sens Environ, 122: 66–74
Homer C, Dewitz J, Yang L, Jin S, Danielson P, Xian G, Megown K. 2015. Completion of the 2011 National Land Cover Database for the conterminous United States—Representing a decade of land cover change information. Photogramm Eng Remote Sens, 81: 345–354
Hutchinson M F. 1995. Interpolating mean rainfall using thin plate smoothing splines. Int J Geogr Inf Syst, 9: 385–403
Ienco D, Interdonato R, Gaetano R, Minh D H T. 2019. Combining Sentinel-1 and Sentinel-2 satellite image time series for land cover mapping via a multi-source deep learning architecture. ISPRS J Photogramm Remote Sens, 158: 11–22
Kattenborn T, Leitloff J, Schiefer F, Hinz S. 2021. Review on Convolutional Neural Networks (CNN) in vegetation remote sensing. ISPRS J Photogramm Remote Sens, 173: 24–49
Kuchler A W, Zonneveld I S. 1967. Vegetation Mapping. Boston: Kluwer Academic Publishers
Li R, Kraft N J B, Yang J, Wang Y. 2015. A phylogenetically informed delineation of floristic regions within a biodiversity hotspot in Yunnan, China. Sci Rep, 5: 9396
Li W, Buitenwerf R, Munk M, Bøcher P K, Svenning J C. 2020. Deep-learning based high-resolution mapping shows woody vegetation densification in greater Maasai Mara ecosystem. Remote Sens Environ, 247: 111953
Liang T G, Feng Q S, Cao J J, Xie H J, Lin H L, Zhao J, Ren J Z. 2012. Changes in global potential vegetation distributions from 1911 to 2000 as simulated by the Comprehensive Sequential Classification System approach. Chin Sci Bull, 57: 1298–1310
Liang W, Abidi M, Carrasco L, McNelis J, Tran L, Li Y, Grant J. 2020. Mapping vegetation at species level with high-resolution multispectral and lidar data over a large spatial area: A case study with Kudzu. Remote Sens, 12: 609
Liu J, Coomes D A, Gibson L, Hu G, Liu J, Luo Y, Wu C, Yu M. 2019. Forest fragmentation in China and its effect on biodiversity. Biol Rev, 94: 1636–1657
Liu Y, Lyu Y, Bai Y, Zhang B, Tong X. 2020. Vegetation mapping for regional ecological research and management: A case of the Loess Plateau in China. Chin Geogr Sci, 30: 410–426
Lopes M, Frison P, Durant S M, Schulte to Bühne H, Ipavec A, Lapeyre V, Pettorelli N, Horning N. 2020. Combining optical and radar satellite image time series to map natural vegetation: Savannas as an example. Remote Sens Ecol Conserv, 6: 316–326
Macintyre P, van Niekerk A, Mucina L. 2020. Efficacy of multi-season Sentinel-2 imagery for compositional vegetation classification. Int J Appl Earth Obs Geoinf, 85: 101980
Madonsela S, Cho M A, Mathieu R, Mutanga O, Ramoelo A, Kaszta Ż, Kerchove R V D, Wolff E. 2017. Multi-phenology WorldView-2 imagery improves remote sensing of savannah tree species. Int J Appl Earth Obs Geoinf, 58: 65–73
Mountrakis G, Im J, Ogole C. 2011. Support vector machines in remote sensing: A review. ISPRS J Photogramm Remote Sens, 66: 247–259
Myers N, Mittermeier R A, Mittermeier C G, da Fonseca G A B, Kent J. 2000. Biodiversity hotspots for conservation priorities. Nature, 403: 853–858
Ni J, Herzschuh U. 2011. Simulating biome distribution on the Tibetan Plateau using a modified global vegetation model. Arctic Antarctic Alpine Res, 43: 429–441
Pedrotti F. 2012. Plant and Vegetation Mapping. Springer Science & Business Media
Preidl S, Lange M, Doktor D. 2020. Introducing APiC for regionalised land cover mapping on the national scale using Sentinel-2A imagery. Remote Sens Environ, 240: 111673
Ran Y H, Li X, Lu L, Li Z Y. 2012. Large-scale land cover mapping with the integration of multi-source information based on the Dempster-Shafer theory. Int J Geogr Inf Sci, 26: 169–191
Räsänen A, Virtanen T. 2019. Data and resolution requirements in mapping vegetation in spatially heterogeneous landscapes. Remote Sens Environ, 230: 111207
Raynolds M K, Walker D A, Balser A, Bay C, Campbell M, Cherosov M M, Daniëls F J A, Eidesen P B, Ermokhina K A, Frost G V, Jedrzejek B, Jorgenson M T, Kennedy B E, Kholod S S, Lavrinenko I A, Lavrinenko O V, Magnússon B, Matveyeva N V, Metúsalemsson S, Nilsen L, Olthof I, Pospelov I N, Pospelova E B, Pouliot D, Razzhivin V, Schaepman-Strub G, Šibík J, Telyatnikov M Y, Troeva E. 2019. A raster version of the Circumpolar Arctic Vegetation Map (CAVM). Remote Sens Environ, 232: 111297
Ren J, Hu Z, Mu X, Zhang P. 1980. Comprehensive sequential classification of grasslands and its genetic significance (in Chinese). Chin Grassl, (1): 12–24
Roberts D W, Cooper S V. 1989. Concepts and techniques of vegetation mapping. In: Ferguson D, Morgan P, Johnson F D, eds. Land Classification Based on Vegetation: Applications for Resource Management. Ogden: USDA Forest Service GTR INT-257. 90–96
Roy P S, Behera M D, Murthy M S R, Roy A, Singh S, Kushwaha S P S, Jha C S, Sudhakar S, Joshi P K, Reddy C S, Gupta S, Pujar G, Dutt C B S, Srivastava V K, Porwal M C, Tripathi P, Singh J S, Chitale V, Skidmore A K, Rajshekhar G, Kushwaha D, Karnatak H, Saran S, Giriraj A, Padalia H, Kale M, Nandy S, Jeganathan C, Singh C P, Biradar C M, Pattanaik C, Singh D K, Devagiri G M, Talukdar G, Panigrahy R K, Singh H, Sharma J R, Haridasan K, Trivedi S, Singh K P, Kannan L, Daniel M, Misra M K, Niphadkar M, Nagabhatla N, Prasad N, Tripathi O P, Prasad P R C, Dash P, Qureshi Q, Tripathi S K, Ramesh B R, Gowda B, Tomar S, Romshoo S, Giriraj S, Ravan S A, Behera S K, Paul S, Das A K, Ranganath B K, Singh T P, Sahu T R, Shankar U, Menon A R R, Srivastava G, Neeti G, Sharma S, Mohapatra U B, Peddi A, Rashid H, Salroo I, Krishna P H, Hajra P K, Vergheese A O, Matin S, Chaudhary S A, Ghosh S, Lakshmi U, Rawat D, Ambastha K, Malik A H, Devi B S S, Gowda B, Sharma K C, Mukharjee P, Sharma A, Davidar P, Raju R R V, Katewa S S, Kant S, Raju V S, Uniyal B P, Debnath B, Rout D K, Thapa R, Joseph S, Chhetri P, Ramachandran R M. 2015. New vegetation type map of India prepared using satellite remote sensing: Comparison with global vegetation maps and utilities. Int J Appl Earth Obs Geoinf, 39: 142–159
Schulz D, Yin H, Tischbein B, Verleysdonk S, Adamou R, Kumar N. 2021. Land use mapping using Sentinel-1 and Sentinel-2 time series in a heterogeneous landscape in Niger, Sahel. ISPRS J Photogramm Remote Sens, 178: 97–111
Senf C, Pflugmacher D, van der Linden S, Hostert P. 2013. Mapping rubber plantations and natural forests in Xishuangbanna (Southwest China) using multi-spectral phenological metrics from MODIS time series. Remote Sens, 5: 2795–2812
Shao Y, Lunetta R S. 2012. Comparison of support vector machine, neural network, and CART algorithms for the land-cover classification using limited training data points. ISPRS J Photogramm Remote Sens, 70: 78–87
Shi H, Chen J. 2018. Characteristics of climate change and its relationship with land use/cover change in Yunnan Province, China. Int J Climatol, 38: 2520–2537
Su Y, Guo Q, Hu T, Guan H, Jin S, An S, Chen X, Guo K, Hao Z, Hu Y, Huang Y, Jiang M, Li J, Li Z, Li X, Li X, Liang C, Liu R, Liu Q, Ni H, Peng S, Shen Z, Tang Z, Tian X, Wang X, Wang R, Xie Z, Xie Y, Xu X, Yang X, Yang Y, Yu L, Yue M, Zhang F, Ma K. 2020. An updated Vegetation Map of China (1:1000000). Sci Bull, 65: 1125–1136
Sun H, Wang J, Xiong J, Bian J, Jin H, Cheng W, Li A, García Mozo H. 2021. Vegetation change and its response to climate change in Yunnan Province, China. Adv Meteor, 2021: 1–20
Tao J, Wen Q, Hua C. 2016. Current status and prospects of primary forest research (in Chinese). Forest Invent Plann, (2): 38–42
Taubert F, Fischer R, Groeneveld J, Lehmann S, Müller M S, Rödig E, Wiegand T, Huth A. 2018. Global patterns of tropical forest fragmentation. Nature, 554: 519–522

Tong X Y, Xia G S, Zhu X X. 2023. Enabling country-scale land cover mapping with meter-resolution satellite imagery. ISPRS J Photogramm Remote Sens, 196: 178–196
Treitz P M, Howarth P J, Suffling R C, Smith P. 1992. Application of detailed ground information to vegetation mapping with high spatial resolution digital imagery. Remote Sens Environ, 42: 65–82
Trisasongko B H, Paull D. 2020. A review of remote sensing applications in tropical forestry with a particular emphasis in the plantation sector. Geocarto Int, 35: 317–339
Tsai Y H, Stow D, Chen H L, Lewison R, An L, Shi L. 2018. Mapping vegetation and land use types in Fanjingshan National Nature Reserve using Google Earth Engine. Remote Sens, 10: 927
Tuanmu M N, Viña A, Bearer S, Xu W, Ouyang Z, Zhang H, Liu J. 2010. Mapping understory vegetation using phenological characteristics derived from remotely sensed data. Remote Sens Environ, 114: 1833–1844
van Beijma S, Comber A, Lamb A. 2014. Random forest classification of salt marsh vegetation habitats using quad-polarimetric airborne SAR, elevation and optical RS data. Remote Sens Environ, 149: 118–129
van der Maarel E, Franklin J. 2012. Vegetation Ecology. New York: John Wiley & Sons
Verrall B, Pickering C M. 2020. Alpine vegetation in the context of climate change: A global review of past research and future directions. Sci Total Environ, 748: 141344
Verrelst J, Camps-Valls G, Muñoz-Marí J, Rivera J P, Veroustraete F, Clevers J G P W, Moreno J. 2015. Optical remote sensing and the retrieval of terrestrial vegetation bio-geophysical properties—A review. ISPRS J Photogramm Remote Sens, 108: 273–290
Wagner F H, Sanchez A, Tarabalka Y, Lotte R G, Ferreira M P, Aidar M P M, Gloor E, Phillips O L, Aragão L E O C, Pettorelli N, Clerici N. 2019. Using the U-net convolutional network to map forest types and disturbance in the Atlantic rainforest with very high resolution images. Remote Sens Ecol Conserv, 5: 360–375
Walker D A, Raynolds M K, Daniëls F J A, Einarsson E, Elvebakk A, Gould W A, Katenin A E, Kholod S S, Markon C J, Melnikov E S, Moskalenko N G, Talbot S S, Yurtsev B A, The other members of the CAVM Team . 2005. The circumpolar Arctic vegetation map. J Veg Sci, 16: 267–282
Wang F, Ding Y, Sayer E J, Li Q, Zou B, Mo Q, Li Y, Lu X, Tang J, Zhu W, Li Z, Gallery R. 2017. Tropical forest restoration: Fast resilience of plant biomass contrasts with slow recovery of stable soil C stocks. Funct Ecol, 31: 2344–2355
Wang X, Yao Y F, Wortley A H, Qiao H J, Blackmore S, Wang Y F, Li C S. 2018. Vegetation responses to the warming at the Younger Dryas-Holocene transition in the Hengduan Mountains, southwestern China. Quat Sci Rev, 192: 236–248
Wu T, Luo J, Gao L, Sun Y, Dong W, Zhou Y, Liu W, Hu X, Xi J, Wang C, Yang Y. 2021. Geo-object-based vegetation mapping via machine learning methods with an intelligent sample collection scheme: A case study of Taibai Mountain, China. Remote Sens, 13: 249
Wu Z, Zhu Y. 1987. Yunnan Vegetation (in Chinese). Beijing: Science Press
Xiahou M, Liu Y, Yang T, Shen Z. 2024. Estimating potential vegetation distribution and restoration in a biodiversity hotspot region under future climate change. J Geogr Sci, 34: 2128–2144
Xie Y, Sha Z, Yu M. 2008. Remote sensing imagery in vegetation mapping: A review. J Plant Ecol, 1: 9–23
Yao Y, Suonan D, Zhang J. 2020. Compilation of 1:50000 vegetation type map with remote sensing images based on mountain altitudinal belts of Taibai Mountain in the North-South transitional zone of China. J Geogr Sci, 30: 267–280
Ye P, Zhang G, Wu J. 2020. Hotspots and conservation gaps: A case study of key higher plant species from Northwest Yunnan, China. Glob Ecol Conserv, 23: e01005
Zeng Y, Gou M, Ouyang S, Chen L, Fang X, Zhao L, Li J, Peng C, Xiang W. 2019. The impact of secondary forest restoration on multiple ecosystem services and their trade-offs. Ecol Indicators, 104: 248–258
Zhang C, Xie Z. 2014. Data fusion and classifier ensemble techniques for vegetation mapping in the coastal Everglades. Geocarto Int, 29: 228–243
Zhang H, Eziz A, Xiao J, Tao S, Wang S, Tang Z, Zhu J, Fang J. 2019. High-resolution vegetation mapping using extreme gradient boosting based on extensive features. Remote Sens, 11: 1505
Zhu Z, Piao S, Myneni R B, Huang M, Zeng Z, Canadell J G, Ciais P, Sitch S, Friedlingstein P, Arneth A, Cao C, Cheng L, Kato E, Koven C, Li Y, Lian X, Liu Y, Liu R, Mao J, Pan Y, Peng S, Peñuelas J, Poulter B, Pugh T A M, Stocker B D, Viovy N, Wang X, Wang Y, Xiao Z, Yang H, Zaehle S, Zeng N. 2016. Greening of the Earth and its drivers. Nat Clim Change, 6: 791–795
Zomer R J, Xu J, Wang M, Trabucco A, Li Z. 2015. Projected impact of climate change on the effectiveness of the existing protected area network for biodiversity conservation within Yunnan Province, China. Biol Conserv, 184: 335–345

(Editorial handling: Jiancheng SHI)